Supplementary figures

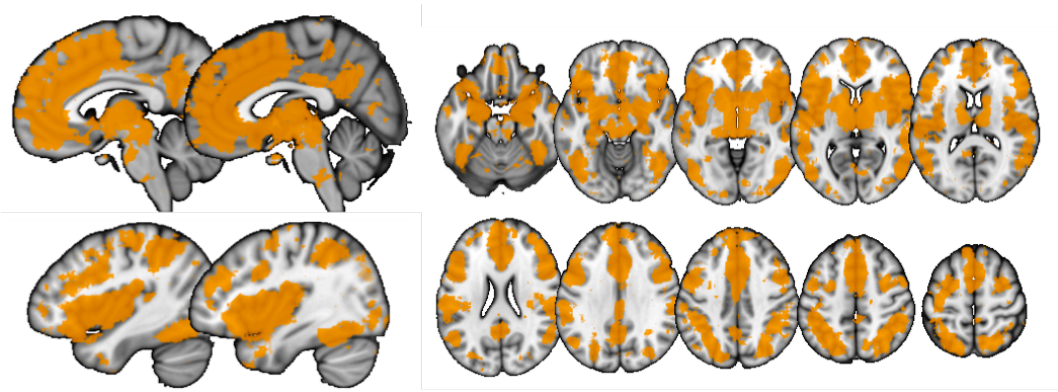

Supplementary Figure 1 (re: Fig. 2 and 3). *A priori* feature selection for global pattern analysis. We constructed a mask of *a priori* voxels associated with 'pain', 'emotion', and 'social' (union of forward and reverse inference) at $q < .1$ FDR-corrected in the Neurosynth database (automated large-scale meta-analytic tool, http://github.com/neurosynth/neurosynth; downloaded on 10/04/2013).

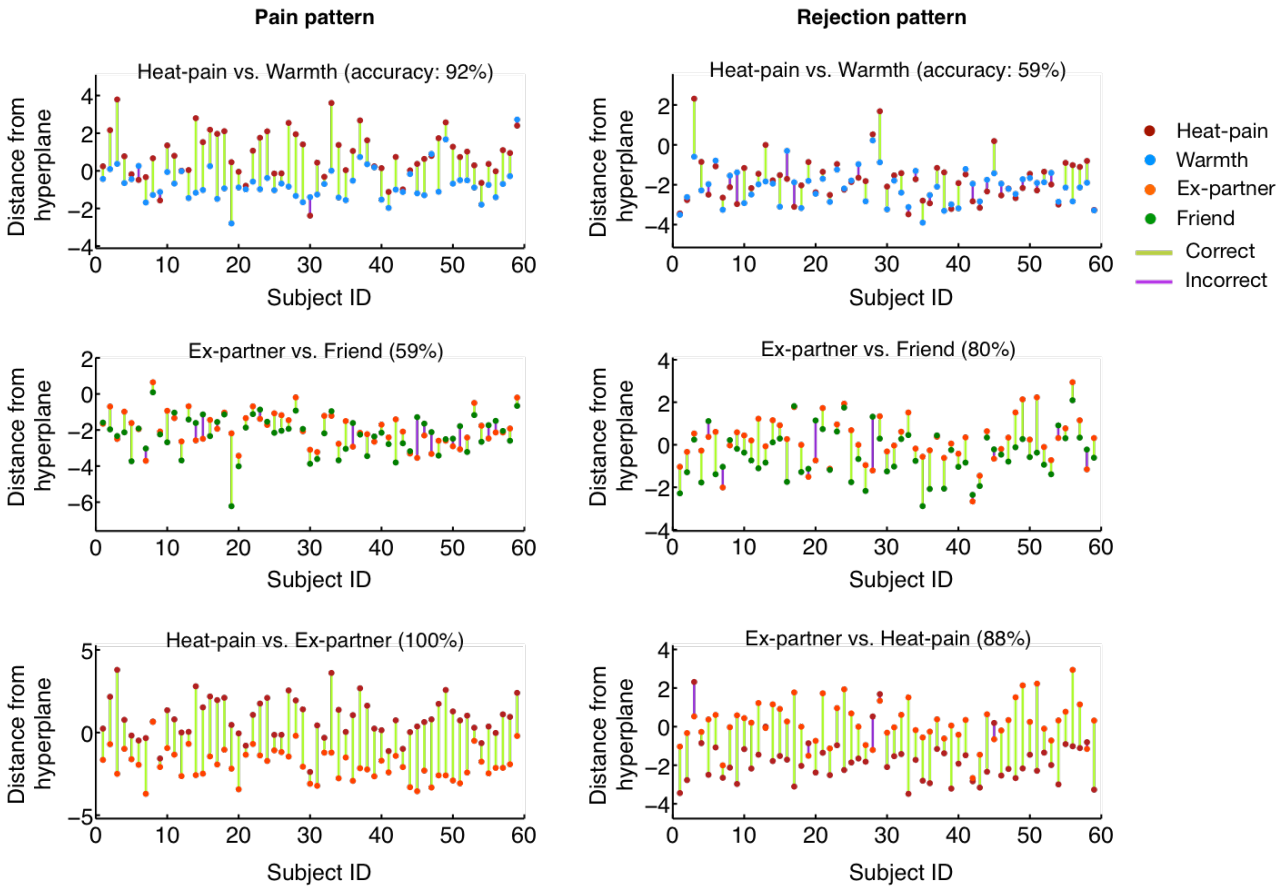

Supplementary Figure 2 (re: Fig. 2). Cross-validated (leave-one-subject-out) distance from hyperplane for each condition and subject. Accuracy was calculated based on forced choice classification for the given contrasts.

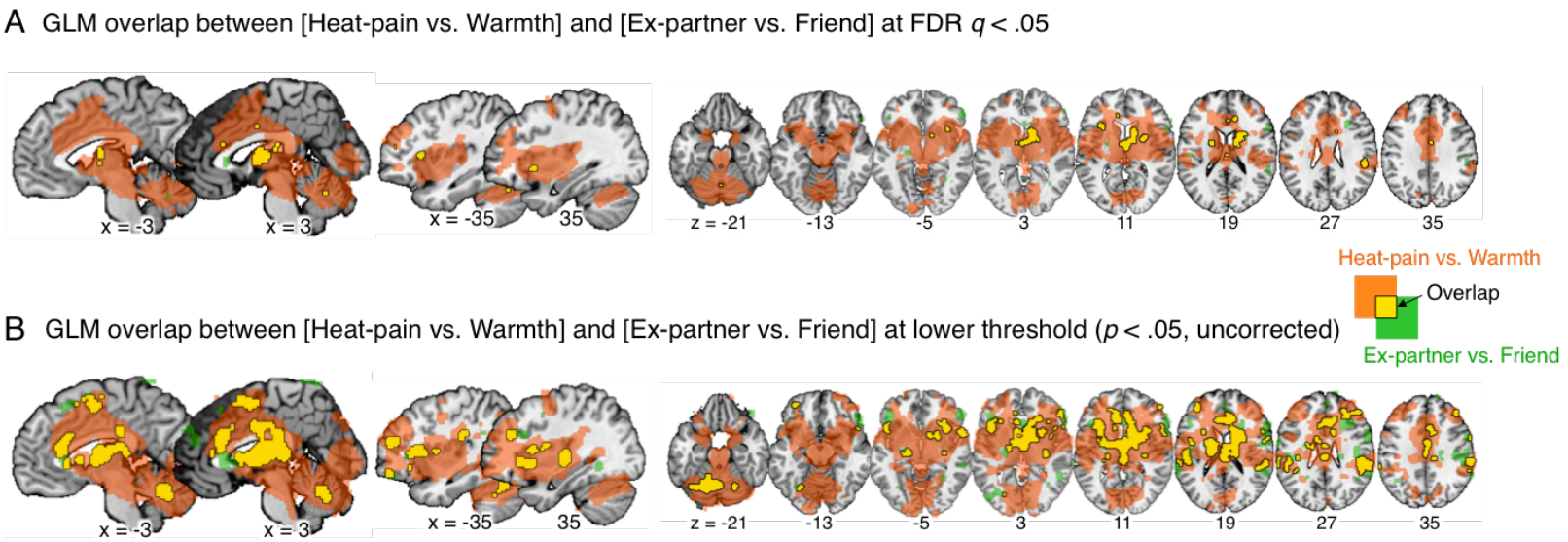

Supplementary Figure 3 (re: Fig. 4). Overlap between [Heat-pain vs. Warmth] and [Ex-partner vs. Friend] contrasts in the general linear model (GLM) analysis. **(A)** FDR-corrected GLM map ($q < .05$). **(B)** Uncorrected GLM map ($p < .05$).

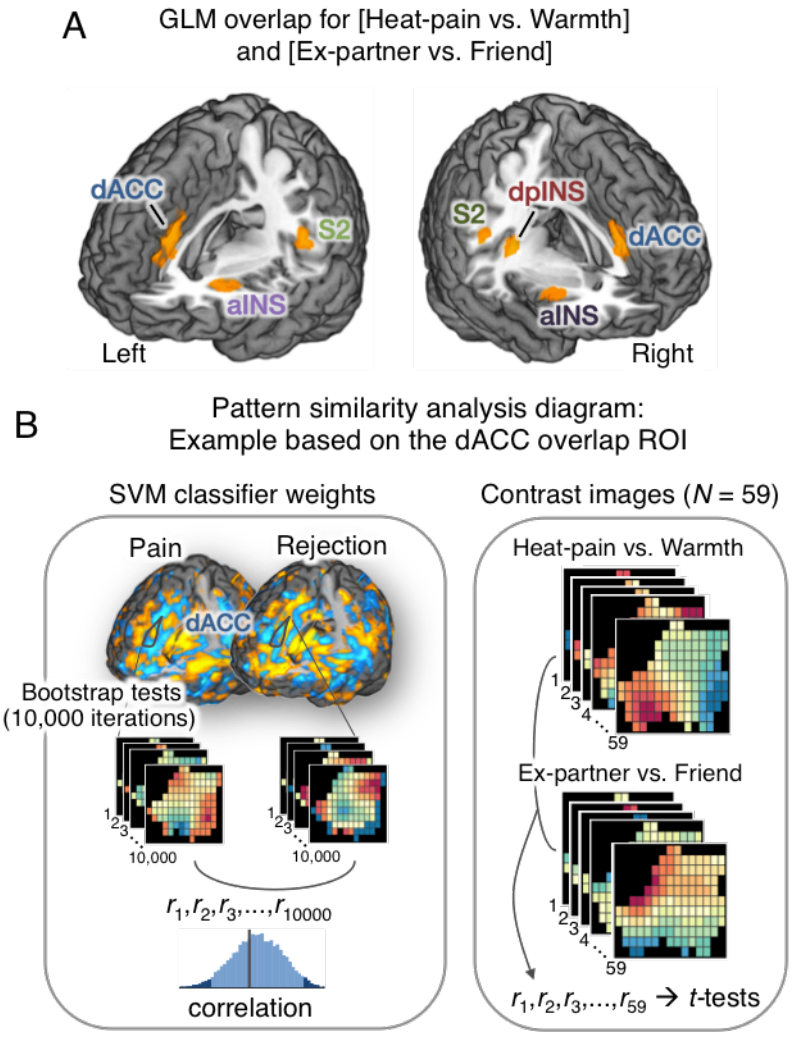

Supplementary Figure 4 (re: Fig. 4). Schematic diagram for multi-voxel pattern similarity analysis for pain-processing regions (A) Regions-of-interest (ROIs) from group-level GLM results. The regions shown here were activated for both [Heat-pain vs. Warmth] and [Ex-partner vs. Friend] and have been implicated in both pain and rejection in prior literature. aINS denotes anterior insula, dACC dorsal anterior cingulate cortex, dpINS dorsal parietal insula. **(B)** Schematic diagram for pattern similarity analysis: Using these ROIs, we extracted data from 1) SVM classifiers for pain and rejection based on bootstrap tests (10,000 iterations) and from 2) subject-level contrast images (one for [Heat-pain vs. Warmth], the other for [Ex-partner vs. Friend]). Then, we vectorized the data and calculated correlations between SVM weights and activation maps for each of the ROIs.

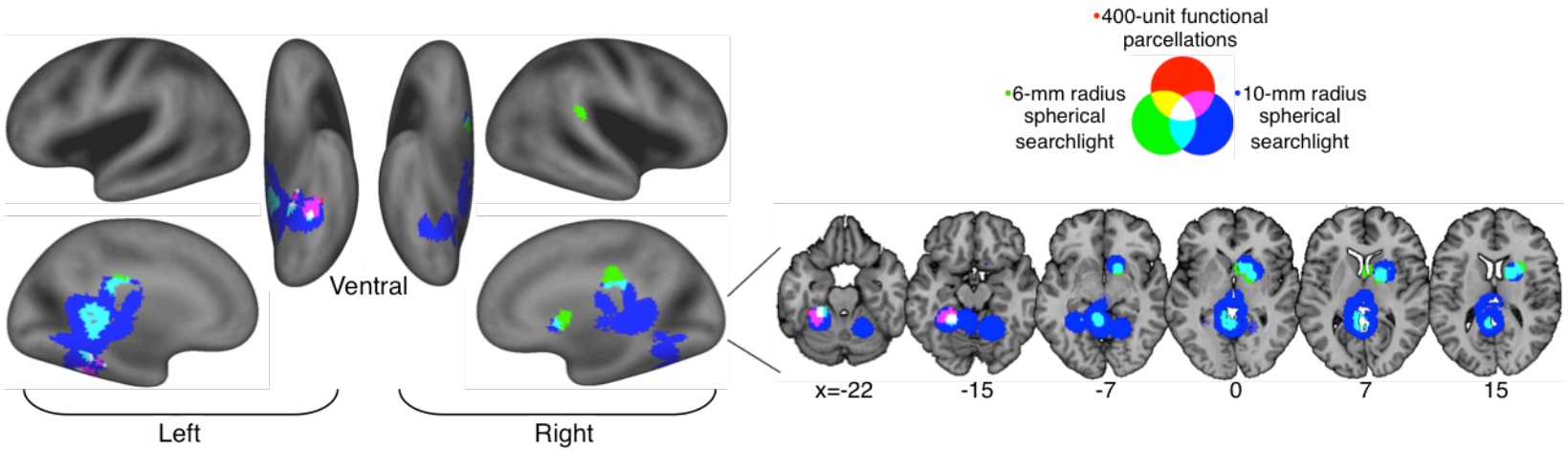

Supplementary Figure 5 (re: Fig. 5). Cross-classification test results with different local region definitions. Given that local pattern analysis can be substantially influenced by the different definitions of local regions (e.g., size of the tested regions), we conducted the same analysis procedure as described in Figure 5 using four different local region definitions, including 200 and 400 functional parcellations[1] and 6- and 10-mm radius spherical searchlights around center voxels. The analyses produced comparable results across all local region definitions, except that no region survived with 200 functional parcellations. We present searchlight results by coloring all the voxels within significant searchlight spheres around center voxels. All results were thresholded at $q < .05$ FDR-corrected.

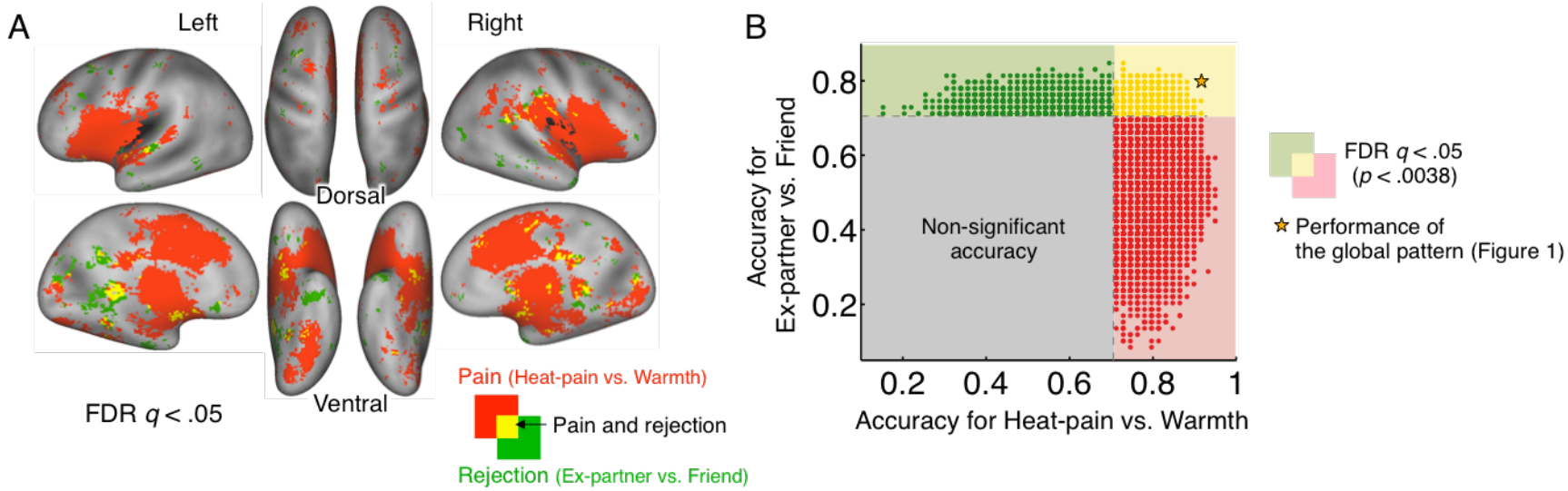

Supplementary Figure 6 (re: Fig. 5). Local pattern analysis results: Within-modality classification accuracy with 6-mm spherical searchlight. (A) The center voxels of the searchlight spheres that accurately discriminated [Heat-pain vs. Warmth] are shown in red while those that accurately discriminated [Ex-partner vs. Friend] are shown in green at $q < .05$ FDR-corrected. **(B)** Scatterplot showing cross-validated, within-modality accuracy for [Heat-pain vs. Warmth] (x-axis) and [Ex-partner vs. Friend] (y-axis) across local regions tested using the searchlight. The star shows the performance of the global pattern from Fig. 1.

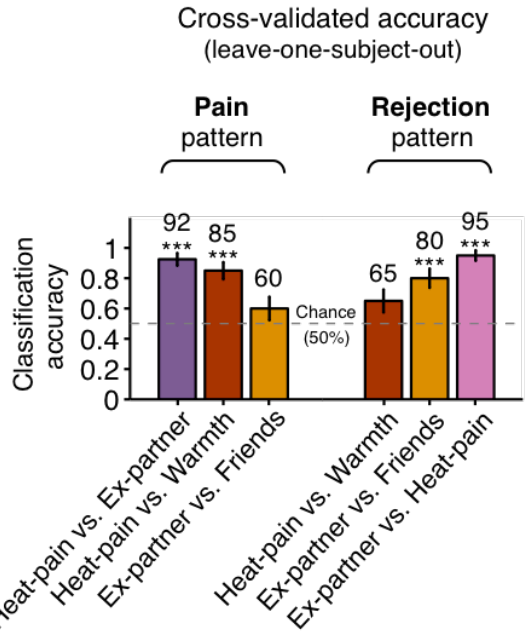

Supplementary Figure 7 (re: Fig. 2). Separate modifiability of fMRI pattern-based classifiers for pain and rejection: Results only with the original dataset (N = 40) used in Kross et al.[2] The plots show cross-validated (leave-one-subject-out) accuracy in two-choice classification tests. The results were similar to the results with the whole dataset (N = 60, Fig. 2A), suggesting the different conclusion between the previous[2] and current study does not result from the addition of 20 more participants, but from the different type of analysis performed (i.e., multivariate pattern analysis). The dashed line indicates the chance level (50%), and the error bars represent standard error of the mean across subjects. $^{***}p < .001$.

Supplementary Table 1. The difference map between the fMRI-pattern based classifiers for pain and rejection.

Regions	x	y	z	voxels	volume (mm^3)
Pain > Rejection					
Superior parietal	24	-70	50	113	904
	-24	-40	44	1	8
	-20	-68	56	48	384
Brainstem	10	-6	-12	57	456
Supramarginal	64	-20	24	8	64
	50	-44	50	20	160
Dorsal posterior insula	40	-8	10	15	120
Parahippocampal	14	-6	-26	15	120
Middle insula	44	-2	-8	13	104
Cerebellum	0	-48	-46	1	8
	32	-60	-30	12	96
Superior temporal (R)	62	-18	6	12	96
Amygdala	-14	-6	-16	12	96
Thalamus	8	-24	2	2	16
Inferior frontal (L)	-46	10	10	6	48
Middle insula (R)	34	6	12	3	24
Occipital	24	-78	20	2	16
Occipital (L)	-24	-82	24	2	16
brainstem	4	-18	-6	1	8
Lingual (R)	12	-74	-2	1	8
	10	-76	0	1	8
Rejection > Pain					
Inferior frontal (L)	-48	22	18	72	576
Perigenual anterior cingulate	-10	36	16	58	464
	-12	30	24	1	8
Ventromedial prefrontal	-10	56	4	54	432
Posterior cingulate	-2	-50	26	50	400
Supramarginal	54	-28	42	38	304
Parahippocampal (L)	-22	-4	-30	24	192
Parahippocampal (R)	22	-16	-24	1	8
Fusiform (L)	-40	-68	-18	13	104
Inferior frontal (R)	52	32	-6	22	176
Lingual (R)	26	-86	-6	21	168
Putamen	-26	-20	0	1	8
	-20	-8	8	19	152
Temporal parietal junction	52	-60	22	17	136
	58	-40	18	4	32
Supplementary motor	0	-14	52	1	8
	-2	24	56	13	104
	-2	-14	56	1	8
Precentral	52	-6	24	1	8
	52	-4	50	6	48
	38	-20	52	1	8
	40	-20	56	3	24
Postcentral	54	-14	40	4	32
	50	-18	44	3	24
Middle frontal	-40	10	48	3	24
Middle temporal (L)	-44	-14	-18	2	16
Middle temporal (R)	50	-14	-16	2	16
Posterior cingulate	2	-44	16	2	16
Cerebellum	30	-36	-32	1	8
Occipital (R)	38	-94	-2	1	8
Occipital (L)	-48	-82	4	1	8
	-44	-70	20	1	8
Inferior frontal (L)	-50	30	2	1	8

Note. We present regions that showed reliable differences between two discriminant weights (SVM weights for pain *minus* SVM weights for rejection) based on bootstrapping of SVMs (10,000 samples) at $q < .05$, FDR corrected.

Supplementary Table 2. Cross-classification test results

	x	y	z	voxels	Volume (mm^3)
Fusiform/parahippocampal	-22	-40	-20	246	1968
Posterior cingulate cortex	2	-30	34	290	2320
Retrosplenial cortex	-4	-46	2	509	4072
Striatum	16	6	10	1045	8360
Temporal parietal junction	64	-30	22	123	984

Note. We present regions that showed significant, cross-classification accuracy in the cross-classification tests with 6-mm radius spherical searchlights around center voxels (the *yellow* colored regions in Fig. 5)

Supplementary References

1 Craddock, R. C., James, G. A., Holtzheimer, P. E., 3rd, Hu, X. P. & Mayberg, H. S. A whole brain fMRI atlas generated via spatially constrained spectral clustering. *Human brain mapping* **33**, 1914-1928, doi:10.1002/hbm.21333 (2012).

2 Kross, E., Berman, M. G., Mischel, W., Smith, E. E. & Wager, T. D. Social rejection shares somatosensory representations with physical pain. *P Natl Acad Sci USA* **108**, 6270-6275, doi:Doi 10.1073/Pnas.1102693108 (2011).